JOURNAL OF MATERIALS SCIENCE 28 (1993) 5917–5921

Indentation, erosion, and strength degradation of silicon-alloyed pyrolytic carbon

P. STRZEPA
CarboMedics, Inc., Austin, TX 78752, USA

E. J. ZAMIROWSKI, J. B. KUPPERMAN*, K. C. GORETTA, J. L. ROUTBORT*
*Materials and Components Technology Division, and *Materials Science Division, Argonne National Laboratory, Argonne, IL 60439, USA*

The effect of sharp particle erosion on the strength and wear of silicon-alloyed pyrolytic carbon was studied. Contact damage at Vickers and Knoop indentations was also examined for comparison with damage at single-particle impact sites. It was found that pyrolytic carbon behaves much differently from most other brittle materials in that even at indentation loads up to 445 N, radial and lateral cracks were not produced. Single-particle impact sites showed a similar lack of radial and lateral crack formation, but did exhibit surface pit formation due to microfracture within, and spalling of, the contact zone. The steady-state erosion rate was similar to that of other polycrystalline ceramic materials. Post-erosion strength and strength variability decreased with increasing particle kinetic energy.

1. Introduction

Silicon-alloyed pyrolytic carbon coatings are extensively used in biomedical prosthetic devices such as mechanical heart valves and orthopaedic joints [1]. Coatings are deposited onto graphite substrates in a fluidized bed process which results in a two-phase microstructure of β-SiC nanocrystals (< 20 nm) uniformly dispersed throughout carbon growth features (grains). The carbon growth features are approximately 1/2 μm diameter and consist of crystallites 2.5–3.0 nm in size having a turbostratic crystal structure [2, 3]. Macroscopically, pyrolytic carbon exhibits isotropic elastic properties and brittle fracture behaviour. Because of the critical lifetime requirements associated with some pyrolytic carbon-coated biomedical devices, its mechanical behaviour is of great interest. The purpose of this study was to examine the effects of solid-particle erosion on the wear and strength of silicon-alloyed pyrolytic carbon. In most brittle materials, erosion damage is in the form of uniform surface microcracks. The response of pyrolytic carbon to these types of microcracks is of importance to its application. Contact damage from Vickers and Knoop indentations was also examined to obtain insight into the response of pyrolytic carbon to sharp indentor contact, and to compare indentation damage with sharp-particle impact damage.

2. Experimental procedure

Specimens of Pyrolite® (CarboMedics, Inc.), a silicon-alloyed pyrolytic carbon, were prepared by coating graphite discs with carbon and sectioning the discs laterally to remove the graphite core. The resultant pieces of Pyrolite carbon were ground and polished to form 1 mm thick by 28 mm diameter discs. On average, specimens contained 7.1 ± 0.3 wt% Si, and had a hardness of 262.1 ± 9.8Hv_{50}, a density of 2.1 g cm^{-3}, a modulus of 27.6 MPa, and Poisson's ratio of 0.2.

Specimens were eroded in the as-polished condition in vacuum at room temperature in a slinger-type erosion apparatus [4]. The erodent was commercial-grade 240-grit size alumina particles having an average particle diameter of 63 μm and density 3.95 g cm^{-3} [5]. Two series of erosion experiments were conducted at normal particle incidence. In the first series of erosion experiments, three sample groups were eroded at 60 m s^{-1} particle velocity. Each group was eroded with a different amount of particles to determine the effect that erodent amount has on strength. The first of these groups was exposed to a very small amount of grit to produce isolated impact sites; the second was exposed to slightly more erodent, resulting in some overlapping impact sites; and the third was eroded well into the steady-state regime. In the second series of erosion experiments, interrupted erosion experiments were conducted until specimens exhibited steady-state erosion rates at particle velocities 40, 60 and 90 m s^{-1}. Erosion rates were determined by weighing the specimens before and after each interruption to an accuracy of ±0.1 mg, and are given here as the ratio W, the mass of material removed per mass of erodent striking the surface. At least five test cycles were performed to define the steady-state erosion rate, which occurs when W is independent of the total mass of impacting particles.

After erosion, all specimens were strength tested in air at room temperature at a crosshead speed of 5 mm min^{-1} with a piston-on-three ball biaxial bending fixture. The support ring radius was

0022–2461

10.96 mm and the loading piston radius was 1.568 mm. Eleven uneroded specimens were tested to establish the strength distribution of the as-polished carbon. The eroded sample groups contained five specimens each.

In addition to the erosion testing, other polished specimens were subjected to static indentations to investigate sharp-indentor contact damage morphology in pyrolytic carbon. Knoop or Vickers microhardness indentors at maximum applied loads of 223, 334, and 445 N were used. During the indentation process, acoustic emission events were monitored with a sonic inspection detector (Hartford Steam Boiler Inspection Technologies Model 204B).

Scanning electron microscopy (SEM) was performed on many of the eroded or indented specimens to characterize the contact damage. In addition, some of the fractured specimens were examined by SEM in an attempt to identify the fracture origins.

3. Results and discussion

3.1. Sharp indentor and impact damage morphology

Scanning electron micrographs in Figs 1 and 2 illustrate contact damage due to static indentations in Pyrolite. The impression due to a Vickers indentation at 445 N is shown in Fig. 1. Inelastic processes occurred beneath the indentor, giving rise to the very faint plastic impression. Several surface cracks are visible at the outer edges of the contact zone. Reflected-light optical microscopy confirmed that while most of these cracks occurred inside the contact zone, a few cracks occurred immediately outside its edge. Steps and ripples on the surface within the contact zone were also observed with optical microscopy. Similar surface cracks and steps, attributed to shear deformation of material beneath the contact zone, have been observed, for example, in soda–lime glass [6, 7]. However, in contrast to other brittle materials, there was no evidence of either radial or lateral crack formation within the pyrolytic carbon at the loads applied.

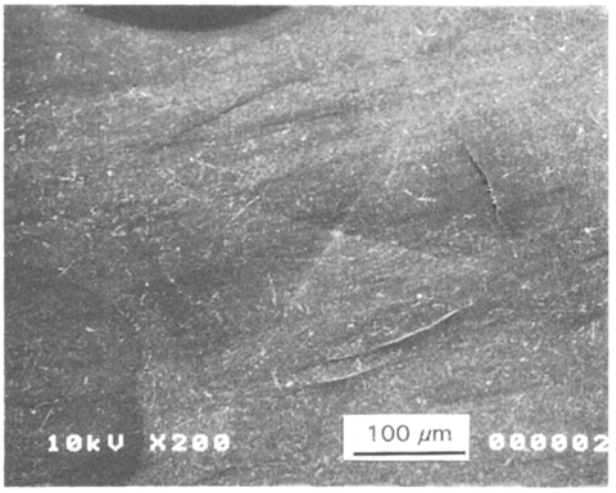

Figure 1 Vickers indentation in pyrolytic carbon (load = 445 N). The plastic impression is very faint. Several surface cracks have formed at the edge of the contact zone. Note the absence of radial and lateral cracks.

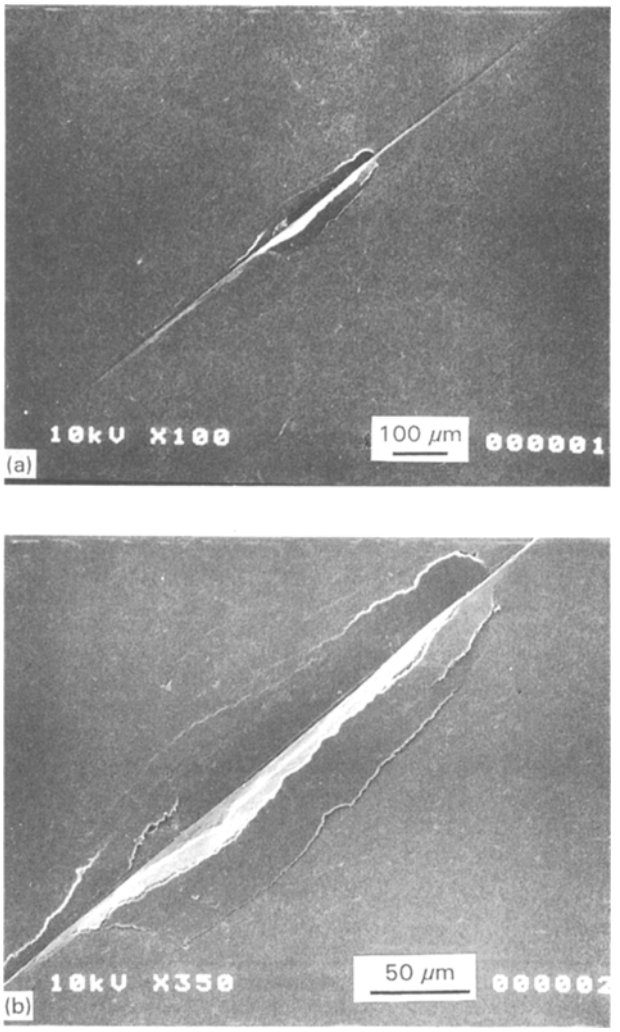

Figure 2 Knoop indentation in pyrolytic carbon (load = 332 N). Surface cracks occur around the central contact zone only. Note the absence of radial and lateral cracks.

A similar damage morphology produced by a Knoop indentation at 334 N can be seen in Fig. 2. The impression due to the Knoop indentor was much more evident compared to the Vickers impression because of the numerous surface cracks at the central contact area (Fig. 2b). Similar to the Vickers indentation, there was no evidence of either radial or lateral crack formation. The surface cracks surrounding the central area of the Knoop impression appear to be lateral cracks because they are the direct cause of surface spalling. Close examination also revealed uplifting of some surfaces surrounding the central contact area, a characteristic feature associated with well-developed lateral cracks [8]. However, two details of this morphology should be emphasized: (1) surface uplift was confined to a small area immediately adjacent to the direct contact zone; and (2) the surface cracks were much smaller than the lateral cracks typically observed at Knoop indentation sites in glass [9] and alumina [10]. Hence, the surface cracks surrounding the Knoop indentation evident in Fig. 2 are not classic lateral cracks, but result from the intense shear deformation and microfracture beneath the indentor [6, 7].

During the indentation process, acoustic emission events increased with increasing load for both indentor types. A single event of significant intensity, such as occurs upon Hertzian ring crack or half-penny crack formation [11], was never observed for the Vickers indentor, even upon unloading. Stable radial or half-penny crack systems could not be produced with either indentor, while many specimens fractured catastrophically during indentation. Fractographic examination of the specimens that failed during Vickers indentation revealed severe microfracture at the contact zone (crushing), cone cracks emanating from the edge of the contact zone, and median cracks directly below the contact zone extending through the specimen thickness (Fig. 3). Note that the median cracks did not exhibit radial crack extensions on the specimen surface. Specimens that failed during Knoop indentation always fractured along a line parallel to the long axis of the indentor. Significant acoustic emissions were recorded during some Knoop indentations in specimens that did not fail, but examination of these impressions revealed only that surface cracks at the edge of the contact zone had fully developed to form a chip of material as shown in Fig. 2b.

When subjected to indentation with a 2.38 mm diameter spherical indentor, pyrolytic carbon displays completely elastic behaviour up to approximately 550 N, when stable cone cracks form [12]. Thus, although this is a very high load, pyrolytic carbon does display the expected response of a brittle material subjected to a blunt indentor. The absence of radial and lateral cracks at sharp indentor contact sites does not eliminate the possibility of elastic/plastic damage behaviour in pyrolytic carbon (see Fig. 3), but indicates that the load threshold for elastic/plastic contact damage is significantly higher in pyrolytic carbon than for other brittle materials. Hence, under low loads, pyrolytic carbon behaves completely elastically even when subjected to sharp indentor contact (which necessitates specialized hardness testing techniques [13]), whereas at moderate loads, pyrolytic carbon exhibits contact damage features observed only at extremely low loads (less than 5 N) in other brittle materials [10]. Relative to solid-particle impact and erosion, the high threshold for elastic/plastic damage of pyrolytic carbon implies that material loss primarily will be due to microfracture within the contact zone leading to the formation of surface pits, and that strength degradation will be determined by the size of the surface pits.

Damage morphology of steady-state erosion surfaces on pyrolytic carbon (Fig. 4) was very similar to that produced on other polycrystalline materials such as alumina [14]. The erosion surface was irregular, and individual impact sites were not apparent. Typical single-particle impact sites are shown in Fig. 5. As anticipated, based on the sharp-indentor results described above, sharp-particle impact damage appears to be confined to the contact zone with little damage visible in the surrounding material. At each impact site, a large amount of material has spalled from the surface to form a 5–10 μm diameter pit. Interestingly, the average pit size did not appear to vary strongly with impacting particle velocity. Small remnants of the contact impression are visible at the edge of each pit. Analogous to the indentation results discussed above, there is no evidence of radial or lateral crack formation at either impact site. Numerous single-particle impact sites with similar features were observed. This type of damage behaviour contrasts strongly with observations for other brittle materials [5, 14–17], but is consistent with the sharp-indentor damage discussed above.

3.2. Erosive wear and strength degradation

For many brittle materials, the steady-state erosion rate, W is related to particle velocity, v, by the power law [17]

$$W \propto v^n \tag{1}$$

where n is the velocity exponent. Fig. 6 illustrates that this functional dependence holds for silicon-alloyed pyrolytic carbon also. A least-squares fit of the data was used to determine that the velocity exponent was $n = 2.6$, the magnitude of which is similar to that

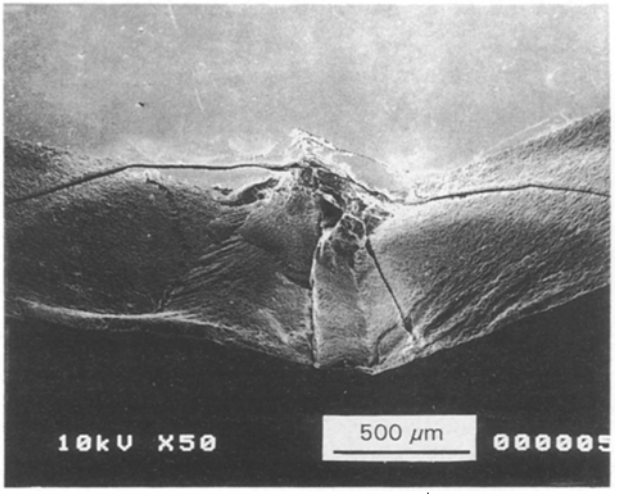

Figure 3 Fracture surface at a 445 N Vickers indentation. Contact zone crushing, a cone crack, and median cracks below the contact zone without radial extensions along the surface are evident.

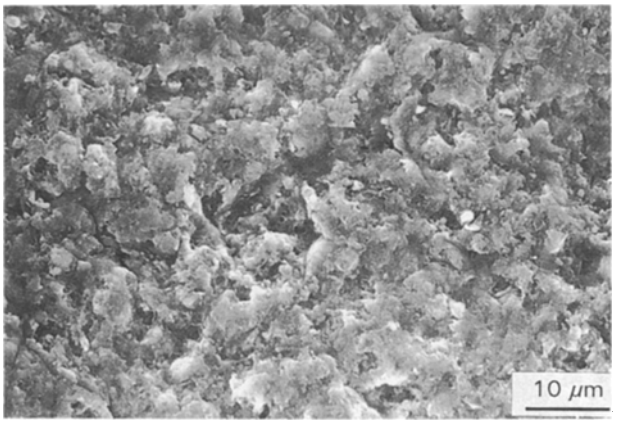

Figure 4 Steady-state erosion surface on silicon-alloyed pyrolytic carbon. Particle kinetic energy = 0.931 μJ.

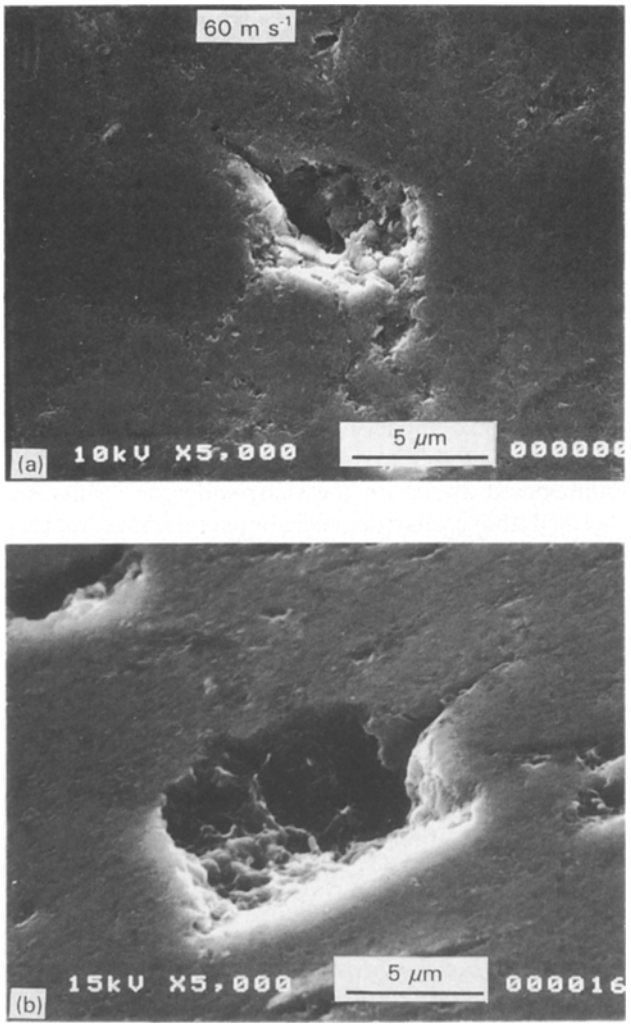

Figure 5 Isolated particle impact sites in silicon-alloyed pyrolytic carbon. Crushing damage is confined to the contact zone. Note the absence of radial and lateral cracks.

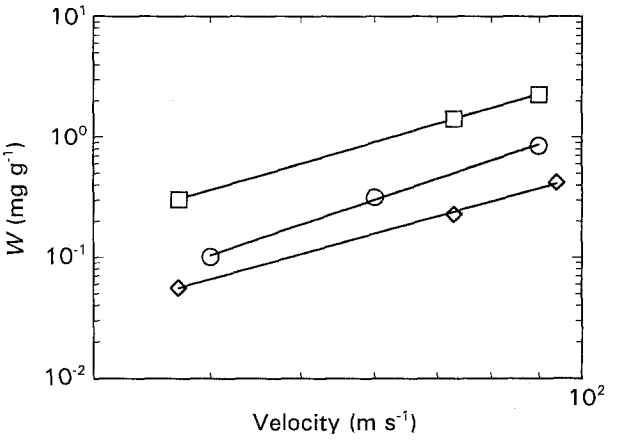

Figure 6 Erosion rate of (○) pyrolytic carbon for particle impact at normal incidence. Velocity exponent is $n = 2.6$. Data for (◇) silicon nitride and (□) alumina are from [18].

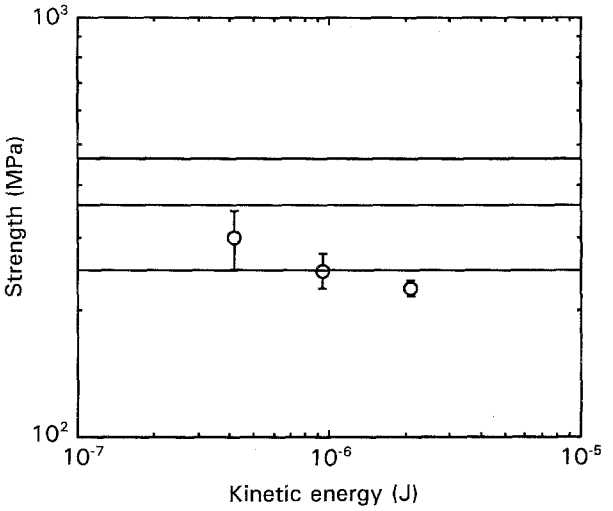

Figure 7 Post-erosion strength behaviour of pyrolytic carbon. The slope of the best-fit line through the data is $\beta = -0.175$. Error bars on data points represent ± one standard deviation; (—) mean ± one standard deviation of the as-polished material.

measured for other brittle materials [17, 18]. Fig. 6 also shows that the erosion-rate magnitude of pyrolytic carbon is very close to other common polycrystalline ceramic materials such as hot-pressed silicon nitride, and polycrystalline alumina [18]. It is noted that the data in Fig. 6 were gathered over similar ranges of kinetic energy [18]. The methods and erodents used were not identical, however, and thus direct comparisons can be only approximate.

Results of strength tests on specimens eroded in the first series of erosion experiments revealed that the post-erosion strength of pyrolytic carbon was not influenced by the amount of erodent striking the specimens. Thus, the strength data of all specimens eroded at the common velocity in that series of experiments were combined. The effect of erodent-particle kinetic energy on mean strength is shown in Fig. 7. As particle kinetic energy increases, decreases were observed both in average strength, and in strength variability. The slope of the best-fit line through the data in Fig. 7 was $\beta = -0.175$. This value agrees well with, but is slightly less than, the $\beta = -0.222$ ($\beta = -2/9$) magnitude predicted based on a quasi-static impact theory [14]. Deviations from the quasi-static impact theory have been observed previously, and are attributable in part to variation of contact conditions or microstructural effects on crack initiation and growth [14, 16, 19, 20].

Although the range of particle kinetic energy utilized in this study was limited, it is interesting to note that strength variability continued to decrease throughout the range of increasing particle energies. Typically, strength variability decreases significantly after erosion because of the new, uniform flaw population generated by the impacting particles, but, in general, the variability is not a function of kinetic energy [21]. Examination of fracture origins on lightly eroded and heavily eroded specimens did not provide evidence that failure resulted from a flaw or pit due to a single impact, or from the linking up of flaws or pits due to multiple impacts. It is possible, however, that all failures resulted from flaw linking, because the possibility of multiple impacts could not be eliminated even in the lightly eroded specimens.

4. Conclusion

Pyrolytic carbon was subjected to indentation and particle-impact damage. This material does not ex-

hibit the radial/lateral crack morphology associated with sharp indentors and angular particles, as is generally observed for brittle materials. Nevertheless, the steady-state erosive wear rates and post-erosion strength behaviour of pyrolitic carbon is similar to those of other brittle materials. In addition, the velocity exponent for erosion and the dependence of the strength on the kinetic energy of impacting erodents are consistent with the quasi-static impact theory. Pyrolytic carbon appears to have a higher threshold for damage than most brittle materials, but experiments need to be performed over a wider range of kinetic energies to confirm this hypothesis.

Acknowledgements

This work was supported by the US Department of Energy (DOE), Basic Energy Sciences-Materials Science, under Contract W-31-109-Eng-38. The work of E. J. S. and J. B. K. was partially supported by the Division of Educational Programs, Argonne National Laboratory, with funding from DOE.

References

1. J. C. BOKROS in "Ceramics in Surgery", edited by P. Vincenzini (Elsevier, New York, 1983) p. 199.
2. J. L. KAAE and T. D. GULDEN, *J. Am. Ceram. Soc.* **54** (1971) 605.
3. J. L. KAAE *Carbon*, **13** (1975) 51.
4. T. H. KOSEL, R. O. SCATTERGOOD and A. P. L. TURNER, in "Wear of Materials 1979", edited by K. C. Ludema, W. A. Glaeser and S. K. Rhee (ASME, New York, 1979) p. 192.
5. K. C. GORETTA, J. L. ROUTBORT, A. MAYER and R. B. SCHWARZ, *J. Mater. Res.* **2** (1987) 818.
6. J. T. HAGAN, *J. Mater. Sci.* **14** (1979) 462.
7. B. R. LAWN, T. P. DABBS and C. J. FAIRBANKS, *ibid.* **18** (1983) 2785.
8. D. B. MARSHALL, B. R. LAWN and A. G. EVANS, *J. Am. Ceram. Soc.* **65** (1982) 561.
9. R. F. COOK and D. H. ROACH, *J. Mater. Res.* **1** (1986) 589.
10. J. LANKFORD, in "Fracture Mechanics of Ceramics", Vol. 6, edited by R. C. Bradt, D. P. H. Hasselman and F. F. Lange (Plenum Press, New York, 1978) p. 245.
11. K. Y. KIM and W. SACHSE, *J. Appl. Phys.* **55** (1984) 2847.
12. J. KEPNER, CarboMedics, Inc., unpublished work (1990).
13. T. M. DEGLEY Jr and B. C. LESLIE, *Nucleonics* **21** (1963) 62.
14. S. M. WIEDERHORN and B. J. HOCKEY, *J. Am. Ceram. Soc.* **62** (1979) 66.
15. J. E. RITTER, P. STRZEPA. K. JAKUS. L. ROSENFELD and K. J. BUCKMAN, *ibid.* **67** (1984) 769.
16. J. E. RITTER, S. R. CHOI, K. JAKUS, R. J. WHALEN and R. G. RATEICK, Jr, *J. Mater. Sci.* **26** (1991) 5543.
17. J. L. ROUTBORT, R. O. SCATTERGOOD and E. W. KAY, *J. Am. Ceram. Soc.* **63** (1980) 635.
18. S. M. WIEDERHORN and B. J. HOCKEY, *J. Mater. Sci.* **18** (1983) 766.
19. K. BREDER, J. E. RITTER and K. JAKUS, *J. Am. Ceram. Soc.* **71** (1988) 1154.
20. R. O. SCATTERGOOD and J. L. ROUTBORT, *ibid.* **66** (1983) C184.
21. P. STRZEPA, MSME thesis, University of Massachusetts, Amherst (1984).

Received 22 September 1992
and accepted 7 May 1993